Development of Chemical Oxygen Demand On-Line Monitoring System Based on a Photoelectrochemical Degradation Principle

ARTICLE *in* ENVIRONMENTAL SCIENCE AND TECHNOLOGY · MAY 2006

Impact Factor: 5.33 · DOI: 10.1021/es052018l · Source: PubMed

3 AUTHORS, INCLUDING:

Shanqing Zhang
Griffith University
122 PUBLICATIONS **2,842** CITATIONS
SEE PROFILE

Huijun Zhao
Griffith University
308 PUBLICATIONS **6,372** CITATIONS
SEE PROFILE

Development of Chemical Oxygen Demand On-Line Monitoring System Based on a Photoelectrochemical Degradation Principle

SHANQING ZHANG, DIANLU JIANG, AND HUIJUN ZHAO*

Centre for Aquatic Processes and Pollution (CAPP) and School of Environmental and Applied Sciences, Gold Coast Campus, Griffith University, PMB 50, Gold Coast Mail Center, Queensland 9726, Australia

A simple, rapid, and sensitive on-line chemical oxygen demand (COD) determination method has been proposed and experimentally validated. The method is based on a photoelectrochemical oxidative degradation principle and operates under a continuous flow mode. The method employs a specially designed thin-layer photoelectrochemical cell that incorporates a highly effective nanoparticulate TiO_2 photoanode. This approach overcomes many problems associated with the conventional COD determination techniques such as long analysis time, consumption of expensive and toxic reagents, production of secondary toxic waste, and poor reproducibility. The effect of important experimental parameters on the analytical signal generation was systematically investigated, and the optimum conditions were obtained. The method was successfully applied to determine the COD of real samples from various industrial wastewaters. The COD value of real samples determined by this method agreed well with the standard dichromate method. The assay time of 1−5 min/sample can be readily achieved. A practical detection limit of 1 mg L^{-1} COD with a linear range of 1−100 mg L^{-1} was achieved under the optimum conditions.

Introduction

Chemical oxygen demand (COD) is one of the most important parameters and has been widely employed for water quality assessment. The standard method for COD determination involves a 2-h analytical procedure under high pressure and temperature (*1*). It also requires the use of expensive (Ag_2SO_4), highly corrosive (H_2SO_4), and toxic ($Cr_2O_7^-$ and $HgSO_4$) reagents (*1*). Consequently, the secondary pollution is unavoidable when the standard method is employed. In addition, the sensitivity of the standard method is approximately 10 mg/L, which is inadequate for many industrial processing control and most environmental monitoring applications. Despite the huge effort in the past, automation of the standard method for on-line, real-time monitoring is still far from satisfactory, especially when rapid and sensitive detections are required (*2*). For the purpose of pollution control, all domestic wastewater treatment plants and many industrial wastewater treatment plants currently require regular oxygen demand analyses. For environmental assessment and management purposes, different levels of government authorities also monitor oxygen demand levels of effluents and natural waterways. The shortfalls of effective on-line rapid techniques mean that end users have, for some time, been desperate for new and improved methods for quantifying oxygen demand. A simpler, more rapid, and sensitive method would be very attractive to end users. It provides a technological base to allow legislative authorities to better regulate and control monitoring practices. It would also be of further interest to these (and other) industries to use such a method for process control and for rapid feedback on the efficiencies of plant operations.

In an attempt to increase the sensitivity and reduce the assay time, many alternative oxidation methods have been investigated. These include microwave-assisted oxidation (*3*), ultrasound-assisted oxidation (*4*), UV−O_3 oxidation (*5*), electrocatalytic oxidation (*6*, *7*), and TiO_2 photocatalytic oxidation (*8*). Among these, the photocatalytic oxidation approach is the most effective degradation method for COD determination due to the superior oxidation ability of illuminated TiO_2. Nevertheless, this type of method does encounter great difficulties in achieving the practical required accuracy, reproducibility, and reliability because the O_2 depletion during the photocatalytic degradation is used as the analytical signal for COD estimation.

Recently, we reported a new COD determination method based on TiO_2 photoelectrocatalytic principle (PeCOD) (*9*−*11*). The new method combined the electrochemical technique with the TiO_2 photocatalysis to achieve direct COD determination. PeCOD method has several advantages over the normal photocatalytic methods. It allows the application of potential bias, which can be used to further increase the photooxidation efficiency due to the suppression of photoelectron and photohole recombination (*12*). The photocurrent originated from the photocatalytic degradation of organics can be directly, sensitively, and accurately measured as an analytical signal for COD determination (*9*−*11*). This method employs a stop-flow operation mode to achieve exhaustive degradation.

This work aims to develop a simple, rapid, and sensitive on-line COD analytical method using continuous flow mode based on the same degradation principle. The method employed a specially designed thin-layer photoelectrochemical detector. The detection principle is proposed and experimentally validated with the model compound, synthetic and real samples. Glucose was employed as the model compound and the synthetic sample used was glucose/glutamic acid (GGA) (*3*). To optimize the system performance, the effects of important experimental parameters on the analytical signal generation were also systematically investigated.

Experimental Section

Materials and Sample Preparation. The indium tin oxide (ITO) conducting glass slides (8 Ω/square) were supplied by Delta Technologies Ltd. Titanium butoxide (97%, Aldrich), sucrose, glucose, glutamic acid, and sodium perchlorate were purchased from Aldrich without further treatment prior to use. All other chemicals were of analytical grade and purchased from Aldrich unless otherwise stated. High-purity deionized water (Millipore Corp., 18 MΩ cm) was used for solution preparation and the dilution of real wastewater samples.

The GGA synthetic samples used for this study were prepared according to the reported method (*3*, *13*). All real samples used for this study were collected from bakeries,

* Corresponding author phone: +61-7-5552 8261; fax: +61-7-5552 8067; e-mail: h.zhao@griffith.edu.au.

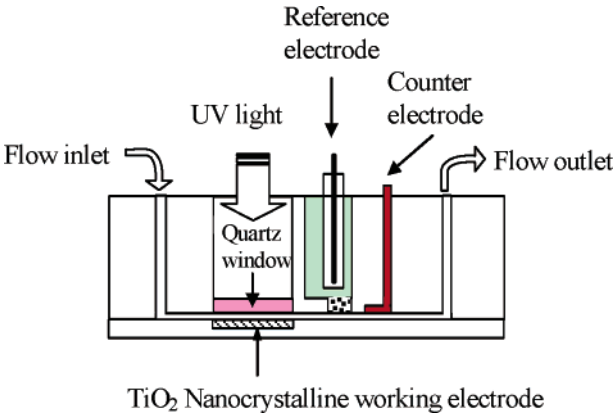

FIGURE 1. Schematic diagram of the photoelectrochemical thin-layer cell for continuous flow analysis.

sugar plants, and breweries, in Queensland, Australia. All samples were preserved according to the guideline of the standard method. When necessary, the samples were diluted to a suitable concentration prior to the analysis. After dilution, the same sample was subject to the analysis by both the standard dichromate COD method and the flow photoelectrochemical COD detector. A certain amount of solid $NaClO_4$ equivalent to 2 M was added to the sample.

Preparation of TiO_2 Electrodes. Aqueous TiO_2 colloid was prepared by hydrolysis of titanium butoxide (*12*). The resultant colloidal solution contains different concentrations of TiO_2 solid with particle sizes ranging from 8 to 10 nm. The procedures for immobilization of TiO_2 colloid onto the ITO conducting substrate were described in our previous papers (*10*, *11*). The coated electrodes were then calcined at 700 °C for 2 h in a muffle furnace. The selection of ITO glass as the conducting substrate was due to its low background electrochemical current, which is essential for sensitive detection.

Apparatus and Methods. All photoelectrochemical experiments were performed at 23 °C in a thin-layer photoelectrochemical cell with a quartz window for illumination (*9*, *10*) (see Figure 1). It consists of a three-electrode system with a TiO_2-coated working electrode. The flow path and the photoelectrochemical reaction zone were confined by a shaped spacer. The thickness of the spacer is 0.2 mm, and the diameter of the quartz lens is 10 mm. A saturated Ag/AgCl electrode and a platinum mesh were used as the reference and counter electrodes, respectively. A voltammograph (CV-27, BAS) was used for application of potential bias. Potential and current signals were recorded using a Macintosh computer (7220/200) coupled to a Maclab 400 interface (AD Instruments). Illumination was carried out using a 150-W xenon arc lamp light source with focusing lenses (HF-200w-95, Beijing Optical Instruments). To avoid the sample solution being heated-up by the infrared light, a UV-band-pass filter (UG 5, Avotronics Pty. Ltd.) was used. Standard COD value (dichromate method) of all the samples was measured with an EPA approved COD analyzer (NOVA 30, Merck).

Results and Discussion

Detection Principle. It is well-known that the UV-illuminated TiO_2 nanocrystallite possesses very strong oxidation power, which is capable of stoichiometrically mineralizing a wide spectrum of organic compounds, due to the photogenerated holes (h^+) (*14*). That is

$$C_yH_mO_jN_kX_q + (2y - j)H_2O \rightarrow yCO_2 + qX^- + kNH_3 + (4y - 2j + m - 3k)H^+ + (4y - 2j + m - 3k - q)e^- \quad (1)$$

where N and X represents a nitrogen and a halogen atom, respectively. The numbers of carbon, hydrogen, oxygen, nitrogen, and halogen atoms in the organic compound are represented by *y*, *m*, *j*, *k*, and *q*, respectively.

When an electrochemical technique is incorporated into a photocatalysis system, namely, photoelectrochemical degradation, the oxidation efficiency can be further improved due to the suppression of photoelectron and photohole recombination by applied potential bias (*9*−*11*). For analytical application, the introduction of electrochemical technique enables the direct measurement of the photocurrent. Under suitable conditions, the photocurrent originated from the photocatalytic oxidation of organics can be obtained and subsequently used as the analytical signal for determination of COD, since it represents the extent of oxidation (*9*−*11*).

The thin-layer photoelectrochemical detector used for this work is a consumption type detector since the organic compounds in the sample are photoelectrochemically oxidized at the TiO_2 working electrode. In our previous works, the exhaustive degradation was achieved by employing a stop-flow operation mode (*9*−*11*). Under these conditions, the amount of electrons captured ($Q_{exhaustive}$) is equal to the theoretical charge ($Q_{theoretical}$) of mineralization of organic compounds in the injected sample and can be expressed by Faraday's Law:

$$Q_{exhaustive} = Q_{theoretical} = FV\sum_{i=1}^{m} n_i C_i \quad (2)$$

where n_i, the oxidation number, refers to the number of electrons transferred for an individual organic compound during the photoelectrocatalytic degradation; C_i is the molar concentration of individual organic compound; and *F* and *V* represent the Faraday constant and the sample volume, respectively.

In the continuous flow mode under controlled conditions, only a portion of the organic compounds in the sample have been degraded. This degraded portion can be represented by α, the oxidation percentage, which is defined as

$$\alpha = \frac{Q_{net}}{Q_{theoretical}} \quad (3)$$

where Q_{net} is the amount of electrons captured during the continuous flow detection, while $Q_{theoretical}$ refers to the theoretical charge required for mineralization of the injected sample.

If all organic compounds can be oxidized indiscriminately, it can be assumed that the oxidation percentage is a constant, which is similar to the situation in a consumption type detection under continuous flow mode (*15*). The amount of electrons captured by the detector can be written as

$$Q_{net} = \alpha FV\sum_{i=1}^{m} n_i C_i \quad (4)$$

Since each oxygen molecule equals to four transferred electrons,

$$O_2 + 4H^+ + 4e^- \rightarrow 2H_2O \quad (5)$$

and according to COD definition, the Q_{net} can be readily converted into equivalent COD value (*9*−*11*).

$$\text{COD (mg/L } O_2) = \frac{Q_{net}}{4\alpha FV} \times 32000 = kQ_{net} \quad (6)$$

Equation 6 can be used to directly quantify the COD value of a sample when Q_{net} is obtained, since *k*, the slope, can be

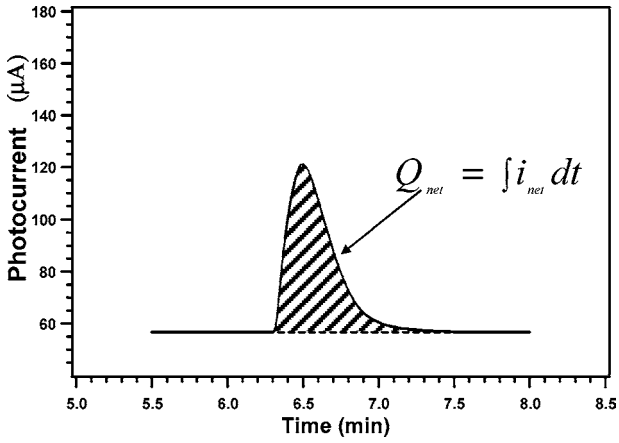

FIGURE 2. Typical photocurrent responses in continuous flow analysis. The shaded area indicates the charge (i.e., Q_{net}) originating from the oxidation of the organic compounds.

obtained by calibration curve method or standard addition calibration method.

Figure 2 shows a typical photocurrent−time profile obtained during the degradation of organic compounds under continuous flow conditions and can be used to illustrate how Q_{net} is obtained. The flat baseline (blank) photocurrent ($i_{baseline}$) observed from the carrier solution is originated from water oxidation, while the peak response observed from the sample injection is the total current of two different components: one is originated from photoelectrocatalytic oxidation of organics (i_{net}), and the other is originated from water oxidation, which was the same as the blank photocurrent. The net charge, Q_{net}, originated from oxidation of organic compounds can be obtained by integration of the peak area between the solid and dashed lines, i.e., the shaded area as indicated in Figure 2.

Thin-Layer Photoelectrochemical Flow Detector. A conventional photoelectrochemical degradation reactor is unsuitable for on-line analytical applications mainly due to its inadequate rapidity (*16*, *17*). For this work, a thin-layer photoelectrochemical detector was specifically designed to suit on-line photoelectrochemical determination of COD under continuos flow conditions (see Figure 1).

The thin-layer configuration is a key feature of the design. Such a configuration is essential for achieving a large (electrode area)/(solution volume) ratio that ensures the rapid degradation of injected sample. It also provides reliable and reproducible hydrodynamic conditions, which is crucial for accuracy, reproducibility, and reliability. In addition, a thin liquid layer benefits the light utilization efficiency because the aqueous media absorbs the UV radiation. Experimental results suggested that 200 μm was the optimum thickness for this application. It was found that a further decrease in the thickness (i.e. 100 μm) causes complications such as uneven flow and high electrical resistance. The latter is of particular concern because it has a significant negative effect on the quality of analytical signal (photocurrent) even when a high concentration of supporting electrolyte (2 M $NaClO_4$) was used.

The performance of the detector is largely determined by the characteristics of the TiO_2-coated working electrode. For this work, a high-temperature-treated (700 °C) electrode was employed for two main reasons. One is due to the strong adhesion between the TiO_2 and the substrate of the electrode, which ensures the mechanical stability. More importantly, the high-temperature-treated electrode tends to degrade a wide spectrum of organic compounds in an indiscriminative manner (*9*−*11*), which is an essential requirement for COD determination.

Light source is another important component, since the effective light intensity is one of the important parameters affecting the degradation rate. For this work, a modified Xenon light source was employed. The output beam was regulated in terms of the size and the intensity of the beam by a group of quartz lenses. A UV-band-pass filter was used to reduce the amount of infrared radiation reaching the detector, which prevents the sample solution from being heated. It should be mentioned that a rear irradiation option was also tested. It was found that over 80% of the irradiated UV component was lost because of the UV absorption of the substrate glass and ITO layer.

Effect of Potential Bias. The photocatalytic degradation efficiency at TiO_2 depends on the degree of recombination of photoelectrons and holes (*18*). To achieve high degradation efficiency, the recombination of photoelectrons and holes must be suppressed. It has been proven that timely removal of photoelectrons from the conduction band is an effective means of minimizing the recombination of photoelectron and hole, because the capture of photoelectrons at the conduction band is often the rate-limiting step of the overall oxidation reaction (*10*, *19*). Potential bias serves as an external driving force removing the photoelectrons from the conduction band to the external circuit and then to the auxiliary electrode where the reduction reaction occurs. On one hand, an optimum potential bias increases the degradation efficiency, and on the other hand, it ensures the maximum photoelectron capture. The latter is of particular interest to us since the magnitude of analytical signal (i.e., Q_{net}) is dependent on the amount of electrons captured. In fact, maximum photoelectron capture is the one of the necessary conditions for obtaining constant α, which is an essential prerequisite for eq 6.

The effect of applied potentials on the net charge, Q_{net}, was investigated. It was found that Q_{net} initially increased with applied potential and then saturated when the applied potential was more positive than +0.25 V. The initial increase of the Q_{net} with applied potential is because the photoelectron removal process is the rate-limiting step of the overall photocatalytic degradation processes (*20*). Under such conditions, an increase in the applied potential results in an increase of the electromotive force. Consequently, more photoelectrons are removed and a larger Q_{net} is obtained. The saturation of Q_{net} at the potentials more positive than +0.25 V is because the process of the photoelectron removal is no longer the rate-limiting step of the overall photocatalytic degradation processes, instead; the interfacial reactions become the rate-limiting step. Under such conditions, the electrons captured are instantly removed (*20*). Therefore, the maximum electron collection efficiency is achieved, and the amount of collected photoelectrons (Q_{net}) is independent of applied potential. The potential bias of +0.3 V vs Ag/AgCl was subsequently selected for the rest of the experiments.

Effect of Flow Rate and Concentration. On the basis of the proposed detection principle, the magnitude of the analytical signal (Q_{net}) is dependent on the total amount of organics oxidized at the electrode. For a given injection volume, the total amount of organics oxidized at the electrode is governed by the flow rate (determining the contact time) and concentration (determining mass transport to the electrode).

According to eq 4, Q_{net} should be directly proportional to the molar concentration. Figure 3 shows the relationship between Q_{net} and the concentration obtained from the degradation of glucose at various flow rates. A linear relationship within the medium concentration range was observed for all flow rates investigated. This indicates the oxidation percentage independent of concentration under these conditions that rationalizes the assumption made for eq 6. It should be mentioned that the analytical linear range

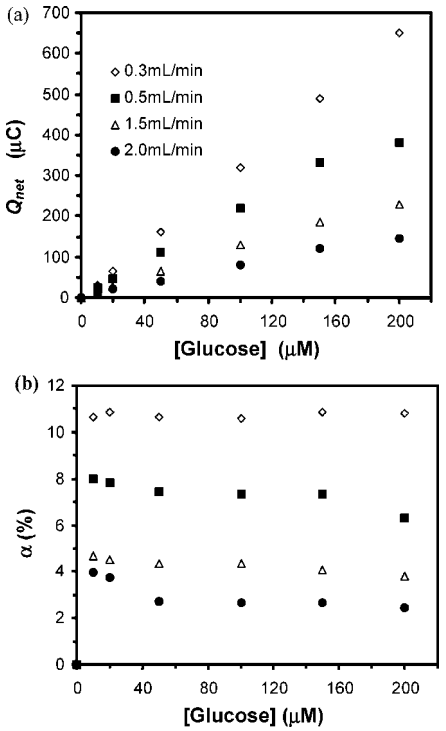

FIGURE 3. Effect of flow rate on the photoelectrochemical charge (a) and the oxidation percentage; (b) The experiments were carried out by the injection of 13 μL of glucose solutions. The carrier was 2 M $NaClO_4$ solution (pH = 7).

decreased as the flow rate increased, which is different from the conventional flow injection detectors, where higher flow rate normally extends the linear range (*21*). It was also observed that the slope of the curve increased as the flow rate decreased. That is, an increase in the flow rate results in a decrease in the sensitivity. This is because a slow flow rate allows longer sample−electrode contact time for the sample to react; therefore, for a given concentration, more charge resulting from the photocatalytic oxidation can be collected.

The rationalization of the assumption made for eq 6 can be further confirmed by the direct relationship between oxidation percentage and concentration (Figure 3b). At a slow flow rate (0.3 mL/min), the oxidation percentage observed was constant throughout the concentration range investigated. However, with higher flow rates, a constant oxidation percentage could be maintained only at higher concentrations (>40 μM glucose), and the fluctuation of the oxidation percentage was observed at low concentrations (<40 μM glucose). The results also confirm that an increase in the flow rate leads to a decrease in the oxidation rate, consequently, the sensitivity of detection. Considering the overall effect of the flow rate, 0.3 mL/min was selected for all subsequent experiments.

Effect of Injection Volume. The injection volume is one of the operational parameters that can strongly influence the detection sensitivity and linear range because it determines the sample contact time under a constant flow rate. Table 1 shows the effect of injection volume on the detection limits and linear range. It was found that when injection volume was increased from 13 to 262 μL, the detection limit was improved from 1 to 0.1 ppm. Despite this improvement on detection limit (sensitivity), too high injection volume can significantly reduce the liner range. This is because the large amount of analytes surpasses the capacity of the photoelectrochemical detector. When this occurs, the oxidation percentage (α) will change with concentration and eq 6 becomes invalid. For this work, a small injection volume

TABLE 1. Effect of Injection Volume on Detection Limit and Linear Range at a Flow Rate of 0.3 mL/min

injection vol (μL)	detection limit (ppm COD)	linear range (ppm COD)
13	1	1−100
36	0.6	1−70
50	0.5	1−50
110	0.2	0.5−40
262	0.1	0.5−20

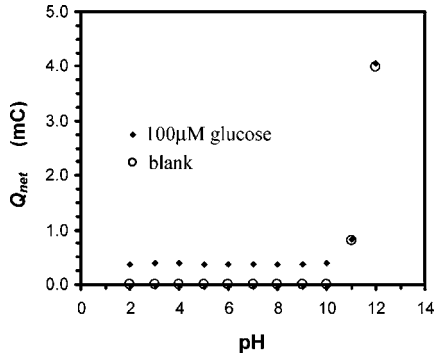

FIGURE 4. Effect of pH on the photoelectrochemical detection of 100 μM glucose: flow rate, 0.3 mL/min; injection volume, 13 μL.

of 13 μL is selected to ensure the validity of eq 6. This injection volume permits the widest linear range (1−100 ppm COD), satisfactory sensitivity, and the detection limit. Additionally, such a small injection volume allows a short assay time.

Effect of pH. Figure 4 shows the effect of pH on the resultant analytical signal (Q_{net}), where all experiments were carried out under identical conditions except pH change. The conditions for pH < 2 were not investigated here because the damage of ITO conductive layer occurs under such acidic conditions. For a given concentration, no significant changes in Q_{net} were observed when the solution pH was varied from 2 to 10. However, a sharp increase in Q_{net} was observed when the solution pH was greater than 10. A question to arise from this observation is whether the sharp increase in Q_{net} is due to increasing oxidation efficiency toward the organics or other factors. To clarify this, the effect of solution pH on the blank current (baseline) was investigated. The blank solutions containing 2 M $NaClO_4$ with various pHs were injected. It revealed that, within the pH range of 2−10, a change in solution pH had no measurable effect on the blank current. A sharp increase in the blank current was observed when the solution pH was greater than 10. Interestingly, the magnitude of the increase matched the value increase observed from the oxidation of glucose. This implies that the increase in Q_{net} at high pH for the case of glucose was due to the increase in the blank current rather than the increase in oxidation efficiency toward glucose. This increase in the blank current (baseline) is due to the increase in water oxidation efficiency at high OH− concentration (*22*, *23*). This suggests that the pH of the sample should be adjusted to the suitable range (pH 2−10) before analysis.

Synthetic Sample Analysis. The applicability of the proposed detection principle was first examined using synthetic samples prepared with pure organic compounds with known theoretical COD value. Figure 5a shows the plot of Q_{net} against synthetic sample concentration in μM. Different slopes for different synthetic samples were observed. It revealed that the slopes decreased in the order of sucrose > GGA > glucose > glutamic acid. This is because the mineralization of different organic compounds require a different number of electrons, $n = 4y - 2j + m - 3k - q$, as described by eq 1. For a given molar concentration, an organic

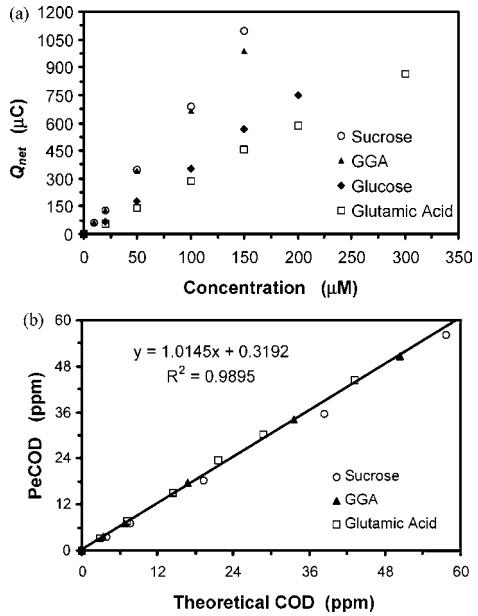

FIGURE 5. Photoelectrochemical determination of COD value of the synthetic samples: (a) Q_{net} − C (μM) relationship; (b) the correlation between the PeCOD and theoretical COD.

compound having a larger n will generate more charge, hence a larger slope, as shown in Figure 5a. The numbers of electrons required for mineralization of 1 mol of the above sample are as follows: sucrose (n = 48 mol) > GGA (n = 42 mol) > glucose (n = 24 mol) > glutamic acid (n = 18 mol), which is in the same order as that of the slopes.

According to eq 6, the measured net charge should be directly proportional to the COD value of the sample. The μM concentration shown in Figure 5a can be converted into the equivalent COD value according to the oxidation number (n). Plotting Q_{net} against the theoretical COD value of the synthetic samples gives a straight line, $y = 19.605x + 1.5887$, $R^2 = 0.999$. This demonstrates that the conversion of the molar concentration of different samples into equivalent COD values is an effective normalization process. For a given sample with known concentration, the theoretical charge ($Q_{theoretical}$) required for mineralization can be readily calculated using eq 2. Therefore, the oxidation percentage (α) can be calculated once the net charge (Q_{net}) of the sample is obtained using eq 3. In Figure 5b, glucose was used as a calibration standard to obtain a slope k. The COD values of the synthetic samples can then be calculated according to eq 6 using the slope k. Figure 5b shows the photoelectrochemical COD (PeCOD) values plotted against theoretical COD values. The trend line of best fit has a slope of 1.0145 with $R^2 = 0.9895$, which demonstrates the applicability of eq 6.

A detection limit of 0.1 ppm COD and a linear range up to 100 ppm COD can be achieved depending on the injection volume and flow rate. The detection limit can be further improved by increasing the sample injection volume, while the linear range can be extended by a further decrease of injection volume. The reproducibility is represented by RSD% = 0.8% that is obtained from 12 repeated injections of 100 μM glucose. The stability was also investigated. Significant baseline shift was observed during the first 2 h when a new electrode was installed. After the baseline is stabilized, no significant change for Q_{net} was obtained from injections of 100 μM glucose over a period of 60 days. The electrode fouling caused by organic contamination and bacteria growth was not observed during the storage due to the well-known merits of self-cleaning ability of TiO_2 (*24*).

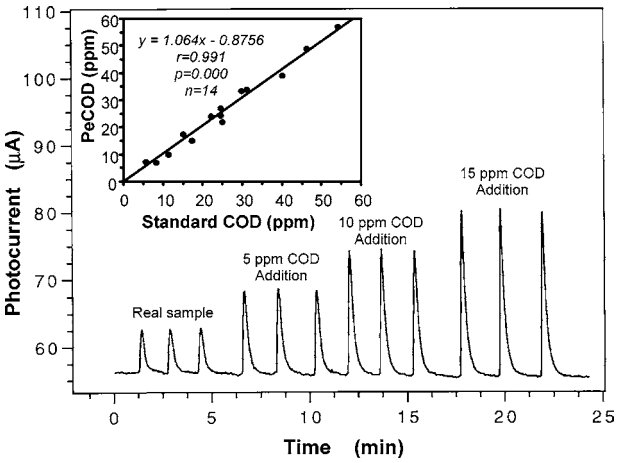

FIGURE 6. Continuous flow photoelectrochemical determination of COD of the real sample using standard addition method. The insert is the correlation between the PeCOD and the standard dichromate COD values for the real samples.

Real Sample Analysis. The applicability of the method for real sample analysis was examined. The pH of the real samples tested in this work was within the range of pH 6−8 (the pH-independent region). Standard addition method was used to determine the COD value in the real sample to eliminate possible signal variation caused by the complex sample matrix. Figure 6 shows the typical photocurrent profile of the continuous flow responses, and the COD value of the real sample was determined using standard addition method.

Each sample was analyzed by both the continuous flow photoelectrochemical method and the standard dichromate method. The insert in Figure 6 shows the correlation between the COD values obtained by both methods. The Pearson correlation coefficient was used as a measure of the intensity of association between the two methods. A highly significant correlation (r = 0.991, P = 0.000, n = 14) between the two methods was obtained, indicating the two methods agreed very well. More importantly, the slope of the principal axis of the correlation ellipse of 1.064 was obtained. The almost identical slope values suggest both methods were accurately measuring the same COD value. Given a 95% confidence interval, this slope was between 1.001 and 1.154. This implies that we can be 95% confident that the true slope lies between these two values. Consider that there are analytical errors associated with measurements performed by both methods and that these errors contribute to scatter on both axes; the strong correlation and almost unity in slope obtained demonstrate the applicability of the continuous flow photoelectrochemical method for determination of chemical oxygen demand.

Acknowledgments

The authors gratefully acknowledge the financial support from Griffith University (Grant GUNRG 2005), Aqua Diagnostic Pty Ltd., Australia, and the Australian Research Council.

Literature Cited

(1) American Public Health Association; American Water Works Association; Water Environment Federation. *Standard methods for the examination of water and wastewater*, 19th ed.; Apha-Awwa-Wef: Washington, D.C., 1995.

(2) Hey, A. E.; Green, A.; Harkness, N. An automated system for the determination of chemical oxygen demand. *Water Res.* **1969**, *3*, 873−886.

(3) Balconi, M. L.; Borgarello, M.; Ferraroli, R.; Realini, F. Chemical oxygen demand determination in well and river waters by flow-injection analysis using a microwave oven during the oxidation step. *Anal. Chim. Acta* **1992**, *261*, 295−299.

(4) Canals, A.; del Remedio Hernandez, M. Ultrasound-assisted method for determination of chemical oxygen demand. *Anal. Bioanal. Chem.* **2002**, *374*, 1132−1140.
(5) Jin, B.; He, Y.; Shen, J.; Zhuang, Z.; Wang, X.; Lee, F. S. C. Measurement of chemical oxygen demand (COD) in natural water samples by flow injection ozonation chemiluminescence (FI−CL) technique. *J. Environ. Monit.* **2004**, *6*, 673−678.
(6) Lee, K.-H.; Ishikawa, T.; McNiven, S.; Nomura, Y.; Sasaki, S.; Arikawa, Y.; Karube, I. Chemical oxygen demand sensor employing a thin layer electrochemical cell. *Anal. Chim. Acta* **1999**, *386*, 211−220.
(7) Lee, K.-H.; Ishikawa, T.; Sasaki, S.; Arikawa, Y.; Karube, I. Chemical oxygen demand (COD) sensor using a stopped-flow thin layer electrochemical cell. *Electroanalysis* **1999**, *11*, 1172−1179.
(8) Kim, Y.-C.; Sasaki, S.; Yano, K.; Ikebukuro, K.; Hashimoto, K.; Karube, I. A flow method with photocatalytic oxidation of dissolved organic matter using a solid-phase (TiO_2) reactor followed by amperometric detection of consumed oxygen. *Anal. Chem.* **2002**, *74*, 3858−3864.
(9) Zhao, H.; Jiang, D.; Zhang, S.; Catterall, K.; John, R. Development of a direct photoelectrochemical method for determination of chemical oxygen demand. *Anal. Chem.* **2004**, *76*, 155−160.
(10) Zhang, S.; Zhao, H.; Jiang, D.; John, R. Photoelectrochemical determination of chemical oxygen demand based on an exhaustive degradation model in a thin-layer cell. *Anal. Chim. Acta* **2004**, *514*, 89−97.
(11) Zhao, H. Photoelectrochemical determination of chemical oxygen demand. Intl. Pat. WO 2004088305, Griffith University, Gold Coast, Australia, 2004.
(12) Jiang, D.; Zhao, H.; Zhang, S.; John, R. Kinetic study of photocatalytic oxidation of adsorbed carboxylic acids at TiO_2 porous film by photoelectrolysis. *J. Catal.* **2004**, *223*, 212−220.
(13) Catterall, K.; Zhao, H.; Pasco, N.; John, R. Development of a rapid ferricyanide-mediated assay for biochemical oxygen demand using a mixed microbial consortium. *Anal. Chem.* **2003**, *75*, 2584−2590.
(14) Matthews, R. W.; Abdullah, M.; Low, G. K. C. Photocatalytic oxidation for total organic carbon analysis. *Anal. Chim. Acta* **1990**, *233*, 171−179.
(15) Ruzicka, J.; Hansen, E. H. *Flow injection analysis*; Wiley: New York, 1981.
(16) Vinodgopal, K.; Stafford, U.; Gray, K. A.; Kamat, P. V. Electrochemically assisted photocatalysis. 2. The role of oxygen and reaction intermediates in the degradation of 4-chlorophenol on immobilized TiO_2 particulate films. *J. Phys. Chem.* **1994**, *98*, 6797−6803.
(17) Byrne, J. A.; Davidson, A.; Dunlop, P. S. M.; Eggins, B. R. Water treatment using nano-crystalline TiO_2 electrodes. *J. Photochem. Photobiol., A* **2002**, *148*, 365−374.
(18) van de Lagemaat, J.; Park, N. G.; Frank, A. J. Influence of electrical potential distribution, charge transport, and recombination on the photopotential and photocurrent conversion efficiency of dye-sensitized nanocrystalline TiO_2 solar cells. A study by electrical impedance and optical modulation techniques. *J. Phys. Chem. B* **2000**, *104*, 2044−2052.
(19) Byrne, J. A.; Eggins, B. R.; Byers, W.; Brown, N. M. D. Photoelectrochemical cell for the combined photocatalytic oxidation of organic pollutants and the recovery of metals from wastewaters. *Appl. Catal., B* **1999**, *20*, L85−L89.
(20) Jiang, D.; Zhao, H.; Zhang, S.; John, R. Characterization of photoelectrocatalytic processes at nanoporous TiO_2 film electrodes: Photocatalytic oxidation of glucose. *J. Phys. Chem. B* **2003**, *107*, 12774−12780.
(21) Zhang, S.; Zhao, H.; John, R. Development of a generic microelectrode array biosensing system. *Anal. Chim. Acta* **2000**, *421*, 175−187.
(22) Rappich, J.; Dohrmann, J. K. The pH dependence of the internal quantum efficiency and of the Peltier heat for photoanodic water oxidation at flame-oxidized titanium: An in situ photoacoustic and photoelectrochemical study. *J. Phys. Chem.* **1989**, *93*, 5261−5264.
(23) Kobayashi, T.; Yoneyama, H.; Tamura, H. Effects of illumination intensity and solution pH on the competitive oxidation of halide ions and water at an illuminated titanium dioxide electrode. *J. Electroanal. Chem. Interfacial Electrochem.* **1981**, *122*, 133−145.
(24) Paz, Y.; Luo, Z.; Rabenberg, L.; Heller, A. Photooxidative self-cleaning transparent titanium dioxide films on glass. *J. Mater. Res.* **1995**, *10*, 2842−2848.

Received for review October 12, 2005. Revised manuscript received January 19, 2006. Accepted January 12, 2006.

ES052018L